Computational Model for an Extendable Robot Body Schema

Alexander Stoytchev
Mobile Robot Laboratory, Georgia Institute of Technology
Atlanta, Georgia 30332-0280 U.S.A.
e-mail: saho@cc.gatech.edu

Technical Report GIT-CC-03-44
October 21, 2003

Abstract

The *body schema* is a perceptually derived model of the body which the brain uses to register the location of sensations on the body and to control body movements. This model of the body is not static and can be extended by noncorporeal objects attached to the body such as clothes, ornaments, and tools. This paper describes a computational model for a *robot body schema* that has extensibility properties similar to its biological analog. The model is based on the model developed by Morasso and Sanguineti (1995) which is modified here to have extendibility properties. The notion of *extended robot body schema* is introduced.

1 Introduction

The sense of body is probably one of the most important senses and yet it is one of the least well studied. It is a complex sense, which combines information coming from proprioceptory, somatosensory, and visual sensors to build a model of the body called the *body schema*. It has been shown that the brain keeps and constantly updates such a model in order to register the location of sensations on the body and to control body movements (Head and Holmes, 1911, Berlucchi and Aglioti, 1997, Berthoz, 2000, Graziano et al., 2002).

Recent studies in neuroscience have shown that this model of the body is not static but can be extended by noncorporeal objects attached to the body such as clothes, ornaments, and tools (Aglioti et al., 1997, Iriki et al., 1996, 2001). Thus, it may be the case that as far as the brain is concerned the boundary of the body does not have to coincide with anatomical boundaries (Iriki et al., 1996, 2001, Tiemersma, 1989).

An important problem that many organisms have to solve early in their developmental cycle is how learn a model of

the sensory stimuli produced by their own bodies. Another important problem is how to relate the capabilities of one's own body to the capabilities of objects that can be attached to the body, i.e., how to discover the affordances of objects (Gibson, 1979).

Many autonomous robots are faced with the same problems (Asada et al., 2001, Yoshikawa et al., 2002). The robotics literature, however, provides few answers to these important problems. This paper attempts to address both of these problems by describing a computational model for a robot body schema that has extensibility properties similar its biological analog. The first problem is addressed by building a sensory motor model of the robot's body that combines visual and proprioceptive information. The second problem is addressed by morphing the body representation of the robot to accommodate the attached object. The robot control algorithms, however, remain unchanged which allows the robot to control the object as if it is controlling its own body.

2 Related Work on Body Schemas

The notion of *body schema* was first suggested by Head and Holmes (1911) who studied the perceptual mechanisms that humans use to perceive their own bodies. They define the *body schema*[1] as a postural model of the body and a model of the surface of the body (Head and Holmes, 1911). It is a perceptual model of the body formed by combining information from proprioceptory, somatosensory, and visual sensors. They suggested that the brain uses such a model in order to register the location of sensations on the body and to control body movements.

Indirect evidence supporting the existence of a body schema comes from numerous clinical patients who experience disorders in perceiving parts of their bodies often lacking sensations or feeling sensations in the wrong place (Frederiks, 1969, Head and Holmes, 1911). One such phenomenon called *phantom limb* is often reported by amputees who feel sensations and even pain as if it was coming from their amputated limb (Melzack, 1992, Ramachandran and Rogers-Ramachandran, 1996).

Direct evidence for the existence of a *body schema* is provided by recent studies which have used brain imaging techniques to identify the specialized regions of the primate (and human) brain responsible for encoding it (Berlucchi and Aglioti, 1997, Iriki et al., 1996, 2001, Graziano et al., 2000). Other studies have shown that body movements are encoded in terms of the body schema (Berthoz, 2000, Graziano et al., 2002). This seems to be the case even for reflex behaviors (Berthoz, 2000).

[1] The exact term that they use is "postural scheme". The term *body schema* was first used by Pick (1922) and was later made popular by Schilder (1923) who published a monograph in German entitled "Das Körperschema".

Perhaps the most interesting property of the body schema is that it is not static but can be modified and extended dynamically in very short periods of time. Such extensions can be triggered by the use of noncorporeal objects such as clothes, ornaments, and tools (Iriki et al., 1996, Tiemersma, 1989). Thus, the body schema is not tied to anatomical boundaries. Instead, the actual boundaries depend on the intended use of the body parts and the external objects attached to the body. For example, when people drive a car they get the feeling that the boundary of the car is part of their own body (Schultz, 2001). However, when they get out of the car their body schema goes back to normal. In some cases, however, it is possible that a more permanent modification of the body schema can be established by objects such as wedding rings that are worn for extended periods of time (Aglioti et al., 1997).

It has been suggested that the pliability of the body schema plays a role in the acquisition of tool behaviors (Head and Holmes, 1911, Paillard, 1993). Recent studies conducted with primates seem to support this hypothesis (Iriki et al., 1996, Berlucchi and Aglioti, 1997, Berti and Frassinetti, 2000). Iriki et al. trained a macaque monkey to retrieve distant objects using a rake and recorded the brain activity of the monkey before, during, and after tool use. They discovered a large number of bimodal neurons (sensitive to visual and somatosensory stimuli) that appear to code the schema of the hand (Iriki et al., 1996). Before tool use the receptive fields (RF) of these neurons were centered around the hand. During tool use, however, the somatosensory RF stayed the same but the visual RF was altered to include the entire length of the rake or to cover the expanded accessible space (Iriki et al., 1996).

This modification of the visual receptive field is limited to the time of tool usage and is conditional upon the intention to use the tool. When the monkey stopped using the tool, or even continued to hold the tool without using it, the visual RF contracted back to normal (Iriki et al., 1996). In a follow up study the monkey was prevented from directly observing its actions and instead was given feedback only through a camera image projected on a video monitor. In this case the visual RF of the bimodal neurons was projected onto the video screen (Iriki et al., 2001).

These studies suggest that the encoding of the body schema in the brain is extremely pliable and tools can easily be incorporated into it. Studies conducted with humans have reached similar conclusions (Berti and Frassinetti, 2000, Farné and Ládavas, 2000). In addition to tools, the body schema can also be modified by prosthetic limbs in amputee patients. These patients can incorporate the prosthetic limb into their body schema in such a way that they can perform the same or similar tasks as if with their real limb (Tsukamoto, 2000).

Unfortunately, little is known about the neural organization of the body schema in primate brains. One recent study, however, has made some quite striking and unexpected discoveries which seem to reject previous theories of the organization of the map of the body and how it is used to control body movements. Graziano et al. (2002) microstimulated the primary

motor and premotor cortex of monkeys at behaviorally relevant time scales (500 ms). Previous studies have already established that stimulation in these areas produces muscle twitches but the stimulation times have always been quite short. The longer stimulation times allowed the true purpose of these areas to be revealed:

> *"Stimulation on a behaviorally relevant time scale evoked coordinated, complex postures that involved many joints. For example, stimulation of one site caused the mouth to open and also caused the hand to shape into a grip posture and move to the mouth. Stimulation of this site always drove the joints toward this final posture, regardless of the direction of movement required to reach the posture. Stimulation of other cortical sites evoked different postures."* (Graziano et al., 2002)

Similar results were obtained not only for hand movements but also for facial expressions: stimulation of a particular site always produced the same final facial expression regardless of the initial facial expression. Similar results were also obtained even when one of the monkeys was anesthetized but the accuracy of the final postures in this case was less precise. Another interesting observation was that obstacles were completely ignored during arm movements induced by microstimulation. If there was an obstacle along the trajectory from the starting posture to the final posture the hand will try to go straight through as if the obstacle did not exist.

These results have led Graziano et al. to conclude that these sites in the primate brain form a coherent map of the workspace around the body. What is even more important, however, is the realization that this map plays an active part in the formation and execution of all kinds of movements. Achieving complex postures involving multiple joints may not be a highly complex task but a consequence of the encoding of this map. Interpolation between different building blocks of this map (i.e., final postures) can be used to produce highly coordinated movements across multiple joints.

Section 3 describes a computational model of a Self-Organizing Body-Schema (SO-BoS) developed by Morasso and Sanguineti (1995) which is adopted and extended in this paper. This model displays similar properties to the observations made by Graziano et al. The equivalent of final postures in Graziano et al.'s paper are called *body icons* in the model of Morasso and Sanguineti (1995). When a body icon is stimulated it acts as an attractor causing the joint configuration of the robot to converge on the one described by the body icon. Extension of SO-BoS model, motivated by the findings of (Iriki et al., 1996), will be introduced in Section 4 to model the extensibility of the Robot Body Schema.

3 Computational Model for a Robot Body Schema

The computational model chosen for the implementation of the RBS is based on the Self-Organizing Body-Schema model introduced in (Morasso and Sanguineti, 1995). This section provides a brief summary of that model and interprets it in terms of existing robotics research.

The method is presented for a robot with M degrees of freedom each with an associated joint angle θ_i. The configuration space, $\mathcal{C}$, of the robot is determined by the Cartesian product of the joint angles:

$$\mathcal{C} \equiv \theta_1 \times \theta_2 \times \ldots \theta_M \subseteq \Re^M$$

Suppose that there are N locations on the body of the robot which can be reliably detected with the robot's sensors. Let $L_R = \{L_{r_1}, L_{r_2}, \ldots, L_{r_N}\}$ be the set of labels referring to these locations. Let each location L_{r_i} have an unique sensory signature S_{r_i}. For each location L_{r_i} there is also a function s_{r_i} which maps the position of L_{r_i} into ego-centric sensor coordinates, i.e.,

$$s_{r_i} : SensorData, S_{r_i} \rightarrow X, Y, Z$$

Let the range of s_{r_i} be the set of three-dimensional vectors $\mathcal{V}_{r_i}$ ($\mathcal{V}_{r_i} \subset \Re^3$) and let v_{r_i} be a specific vector in this space. The sensor space $\mathcal{S}$ of all sensory stimuli coming from the robot's body is given by the Cartesian product of all $\mathcal{V}_{r_i}$

$$\mathcal{S} \equiv \mathcal{V}_{r_1} \times \mathcal{V}_{r_2} \times \ldots \mathcal{V}_{r_N}$$

The main idea behind the SO-BoS model is to link the configuration space and the sensor space of the robot into one $\mathcal{CS}$-space.

$$\mathcal{CS}\text{–}space = \mathcal{C} \times \mathcal{S}$$

The $\mathcal{CS}$-space can be used to identify the current robot configuration as well as to plan robot movements. Previous approaches described in the robotics literature have noted the usefulness of this space for planning and specifying robot movements (Hervé et al., 1991, Sharma et al., 1992, Sharma and Sutanto, 1996). However, they have used algebraic techniques to express this space as an (M+N)-dimensional manifold which is hard to use even for simple robots (Sharma and Sutanto, 1996). The current approach uses non-parametric statistical techniques to approximate the $\mathcal{CS}$-space.

Let $\mu = [\theta_1, \theta_2, \ldots, \theta_M]$ represent a joint angle vector and let $\tilde{\mu}_i = \left[\tilde{\theta}_1^i, \tilde{\theta}_2^i, \ldots, \tilde{\theta}_M^i\right]$ ($\tilde{\mu}_i \in \mathcal{C}$) be a specific instance of this vector. Let $\beta = [v_{r_1}, v_{r_2}, \ldots, v_{r_N}]$ be a vector which represents the coordinates of body locations L_{r_1} through L_{r_N} in sensor space. Also, let $\tilde{\beta}_i = \left[\tilde{v}_{r_1}^i, \tilde{v}_{r_2}^i, \ldots, \tilde{v}_{r_N}^i\right]$ ($\tilde{\beta}_i \in \mathcal{S}$) be a specific instance of this vector.

The body schema model is built around the concept of a *body icon* which is a pair of vectors $(\tilde{\mu}_i, \tilde{\beta}_i)$ representing the motor and sensory components of a specific joint configuration of the robot. A large number of empirically learned body icons, $\left[(\tilde{\mu}_i, \tilde{\beta}_i), i = 1, \ldots, \mathcal{I}\right]$, is used to approximate the $\mathcal{CS}$-space. It is believed that the brain uses a similar representation encoded as a cortical map (Morasso and Sanguineti, 1995, Graziano et al., 2002).

The main building blocks of the SO-BoS model are processing elements (PEs) which have an activation function U_i and a preferred body icon $(\tilde{\mu}_i, \tilde{\beta}_i)$. The body icons are learned from self-observation data gathered while performing random joint movements using the algorithm described in (Morasso and Sanguineti, 1995). The activation function of each PE is determined by the normalized gaussian or softmax function,

$$U_i(\mu) = \frac{G(\|\mu - \tilde{\mu}_i\|)}{\sum_j G(\|\mu - \tilde{\mu}_j\|)} \tag{1}$$

where G is a gaussian function of equal variance and zero mean, μ is the current joint angle configuration, and $\tilde{\mu}_i$ is the motor component of the preferred body icon for this PE. The variance, σ^2, of the gaussian function G is the same for all PEs and its magnitude determines the size of their receptive fields. If σ^2 is small then a PE will be activated only if its preferred motor vector $\tilde{\mu}_i$ is close to the current joint vector μ. If σ^2 is large then more PEs will be activated for any specific joint configuration μ.

The motor-sensory mapping (or forward kinematics) is explicit for motor vectors which are the same as one of the $\tilde{\mu}_i$ prototypes in the learned body icons (i.e., $\tilde{\beta}_i$ can be obtained directly from the sensory component of the same body icon). For an arbitrary joint vector μ ($\mu \neq \tilde{\mu}_i, i = 1, \ldots, \mathcal{I}$) the corresponding β vector can be approximated with the following formula (Morasso and Sanguineti, 1995),

$$\beta^{approx}(\mu) \approx \sum_i \tilde{\beta}_i U_i(\mu) \tag{2}$$

which can be interpreted as a minimum variance estimator. Thus, the forward model $\beta = \beta(\tilde{\mu})$ can be approximated for any joint vector using Formula 2. This formula can also be interpreted as a two step approximation algorithm using *look up* and *interpolation*. The first step looks up the most highly activated PEs for the given joint angle μ. The second step sums the $\tilde{\beta}_i$ vectors of these PEs (scaled by their activation value U_i) to approximate $\beta(\mu)$.

3.1 Achieving Goal Directed Movements

This body schema representation can also be used for control of goal directed movements. The idea is to specify the robot movements in $\mathcal{S}$-space, but carry the movements in $\mathcal{C}$-space. The body schema representation allows that without the need for inverse kinematics transformations because the two spaces are combined into one in the form of body icons.

The learning algorithm described in (Morasso and Sanguineti, 1995) guarantees that each processing element has a neighborhood of other processing elements whose body icons are similar to its own. This similarity is both in terms of their μ and β vectors as well as their activation levels for a fixed joint vector (Morasso and Sanguineti, 1995). This locality property can be exploited to implement a gradient ascent strategy for moving the robot from one configuration to another.

The gradient ascent is carried out in a potential field ξ in which the location of the target has a maximum value and all other points are assigned values in proportion to their distance from the target. The potential field is imposed on the $\tilde{\mu}_i$ components of all PEs but is computed based on the $\tilde{\beta}_i$ components and their distance to the goal in $\mathcal{S}$-space. The calculation of the potential field is similar to the motor schema approach to robot control (Arkin, 1998). In this case, however, the potential field is discretized across all PEs. Each PE_i is assigned a value $\tilde{\xi}_i$ which is a sample of the magnitude of the potential field. The global potential field can be approximated using the following equation:

$$\xi(\mu) \approx \sum_i \tilde{\xi}_i U_i(\mu) \tag{3}$$

Taking advantage of the locality property of the PE array and the form of the softmax activation function, the gradient ascent strategy can be achieved with only local computation (Morasso and Sanguineti, 1995),

$$\dot{\mu} = \gamma \sum_i (\tilde{\mu}_i - \mu)\tilde{\xi}_i U_i(\mu) \tag{4}$$

4 Extending the Robot Body Schema

The RBS model described in the previous section is not pliable, i.e., it is not affected by objects attached to the robot. This section modifies that model to have extensibility properties similar to the biological body schema. The extension of the RBS by an object should be subject to three conditions: 1) there must be a physical contact with the object; 2) there must be a motivation to use the object (i.e., just touching an object during a collision should not trigger an extension); and 3) there must be perceptual and computational routines to update the RBS model to incorporate the object and thus produce the *Extended Robot Body Schema* (ERBS). This extension process is shown on Figure 1.

The main idea behind the extension method presented here is to add offset vectors to the sensory components of all body icons. Thus, the *extended body icons* have the form $< \tilde{\mu}_i, \tilde{\beta}_i + \mathit{offset}_i >$. In order to achieve this extension the sense of touch will be used. This is a natural choice because touch plays an important role in the extension of the body schema in primates (Iriki et al., 1996). As before, let $L_R = \{L_{r_1}, L_{r_2}, \ldots, L_{r_N}\}$ be the set of robot body locations and let $C = \{C_{r_1}, C_{r_2}, \ldots, C_{r_N}\}$ be the set of contact (or touch) sensors associated with these locations. Let each contact sensor,

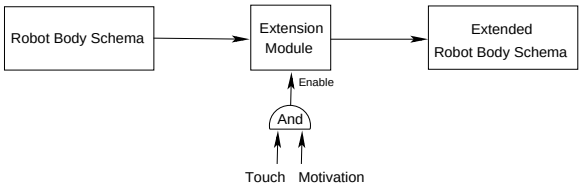

Figure 1: The extension of the robot's body schema is conditional upon touch sensations produced by the object when it is grasped as well as motivation to use the object.

C_i, have an activation function, c_i, which returns a binary value according to the following activation function

$$c_i = \begin{cases} 0 & : \quad if \ F_{C_i} < F_t \\ 1 & : \quad otherwise \end{cases}$$

where F_t is a threshold value (one and the same for all C_i) and F_{C_i} is the magnitude of the contact force applied at C_i.

For the sake of explanation, assume that only one contact sensor is triggered whenever an object is attached to the robot. Let this sensor be C_{r_j} and let its corresponding body location be L_{r_j} (this location will be referred to as the attachment point). Furthermore, assume that the attached object has only one location, L_{ob}, that can be detected by the robot's sensors and let v_{ob} represent its coordinates in ego-centric sensor space. Now the RBS can be extended by adding offset vectors to the sensory components of all body icons that correspond to the attachment point. In other words,

$$\tilde{v}^i_{r_j} = \tilde{v}^i_{r_j} + offset^i_{r_j} \tag{5}$$

The offset vectors effectively shift the centers of the visual receptive fields of the body icons. Once the extended body icons are calculated the position of L_{ob} can be controlled using the potential field method described in Section 3.1. The offset vectors are computed continuously which allows the RBS to be extended dynamically. For example, if the object is re-grasped the position of L_{ob} relative to the attachment point will change and so will the extended body icons. The same holds true if another location on the object is chosen for the extension.

The magnitudes of the offset vectors are the same for all body icons. They are equal to the distance between the position of the object location, v_{ob}, and the position of the attachment point, v_{r_j}. The orientations of the offset vectors, however, are different for all body icons since they depend on the joint configuration of the robot. Because the body icons already contain the positions of all body locations for different joint angles the offset vectors will be expressed in terms of these stored positions. This approach simplifies the calculations needed to extend the RBS.

The idea is to express the offset vectors in a coordinate system that is centered at the attachment point (Figure

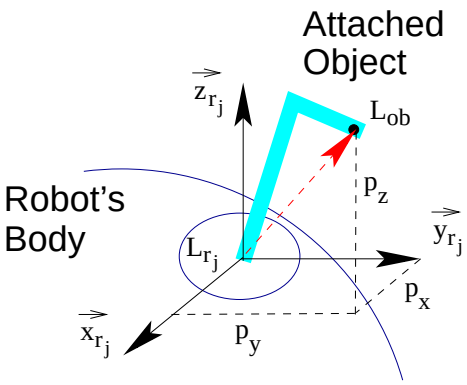

Figure 2: The offset vector is expressed in a coordinate system centered at the attachment point L_{r_j}. See text for details.

2). The basis vectors of this coordinate system, $\vec{x}_{r_j}$, $\vec{y}_{r_j}$, and $\vec{z}_{r_j}$, are chosen so that they are expressible in terms of the positions of the body locations of the robot. In other words, $\vec{x}_{r_j} = f(v_{r_1}, v_{r_2}, \ldots, v_{r_N})$, $\vec{y}_{r_j} = g(v_{r_1}, v_{r_2}, \ldots, v_{r_N})$, $\vec{z}_{r_j} = h(v_{r_1}, v_{r_2}, \ldots, v_{r_N})$. The problem of how the basis vectors can be identified and learned automatically is left for future work. The offset vector for the current joint configuration of the robot can be expressed as: $offset_{r_j} = p_x\vec{x}_{r_j} + p_y\vec{y}_{r_j} + p_z\vec{z}_{r_j}$. The scalars p_x, p_y, and p_z can be obtained by projecting the offset vector onto the three basis vectors (Figure 2).

In order to compute all offset vectors the basis vectors, $\vec{x}^i_{r_j}$, $\vec{y}^i_{r_j}$, and $\vec{z}^i_{r_j}$ should be computed for all joint configurations stored in the body icons. These vectors are given by

$$\vec{x}^i_{r_j} = f(\tilde{v}^i_{r_1}, \tilde{v}^i_{r_2}, \ldots, \tilde{v}^i_{r_N}), \qquad \vec{y}^i_{r_j} = g(\tilde{v}^i_{r_1}, \tilde{v}^i_{r_2}, \ldots, \tilde{v}^i_{r_N}), \qquad \vec{z}^i_{r_j} = h(\tilde{v}^i_{r_1}, \tilde{v}^i_{r_2}, \ldots, \tilde{v}^i_{r_N})$$

Thus, the offset vectors are given by

$$offset^i_{r_j} = p_x\vec{x}^i_{r_j} + p_y\vec{y}^i_{r_j} + p_z\vec{z}^i_{r_j}$$

5 Experiments

The ideas presented in Section 4 were tested with a simulation of a two-dimensional manipulator arm with two rigid limbs and two rotational joints (Figure 3a). The limbs have lengths l_1 and l_2 and the joints can be rotated independently at angles θ_1 and θ_2. Both joints can rotate only 180 degrees, i.e., $0 \leq \theta_1, \theta_2 \leq \pi$. The free end of the second limb has a gripper which can be used to grab objects. The robot also has a camera which can observe the movements of the limbs.

The robot has two body locations, L_{r_1} and L_{r_2}, associated with the joint between the two limbs and the free end of

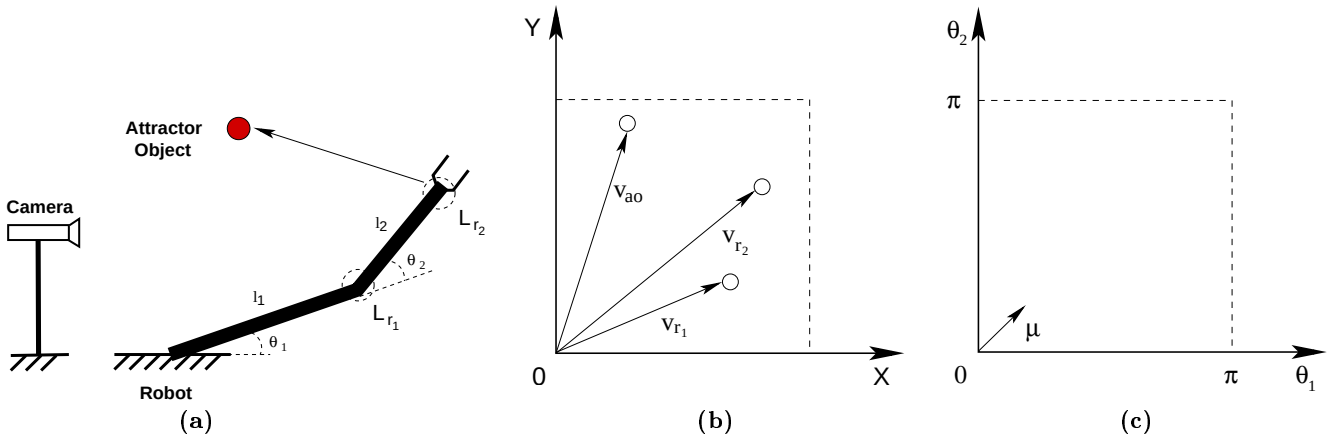

(a) (b) (c)

Figure 3: (a) The two joint robot used in the experiments. The robot has two body locations L_{r_1} and L_{r_2} and two joint angles θ_1 and θ_2. (b) The coordinates of the two body locations in visual space are given by the two vectors v_{r_1} and v_{r_2}. The coordinates of the attractor object are given by the vector v_{ao}. (c) The motor vector, μ, for the robot configuration shown in a).

the second limb (Figure 3a). Their coordinates in sensor space are given by the vectors v_{r_1} and v_{r_2}. Both v_{r_1} and v_{r_2} lie in a two-dimensional space XY defined by the camera image (Figure 3b). The sensory vector β is given by $\beta = \{v_{r_1}, v_{r_2}\}$. An attractor object (AO) is placed in the robot environment and its coordinates are given by the vector v_{ao}. The motor (or joint) vector is given by $\mu = \{\theta_1, \theta_2\}$ (Figure 3c).

The parameters of all PEs in the body schema representation can be computed automatically using the algorithm presented in (Morasso and Sanguineti, 1995). Figure 4a shows the $\tilde{v}^i_{r_1}$ components of the sensory vectors $\tilde{\beta}_i$ for all body icons (i.e.,$i = 1 \ldots \mathcal{I}$). These points belong to the $\mathcal{V}_{r_1}$ sensor space which represents the set of all possible positions of the "elbow" joint. Similarly, Figure 4b shows the positions of the $\tilde{v}^i_{r_2}$ components of all sensory vectors $\tilde{\beta}_i$. These points belong to the $\mathcal{V}_{r_2}$ sensor space which represents the set of all possible end effector positions[2].

The first experiment involved reaching toward an attractor object placed in the environment around the robot. The task of the robot was to touch the attractor object with its end effector. As described in Section 3.1, this task can be solved with a gradient ascent strategy (Equation 4) carried out in a potential field. The potential field is specified as an

[2]These results were obtained after fifteen epochs of the learning algorithm (Morasso and Sanguineti, 1995) with $\mathcal{I}$=400 body icons. The initial values of the learning rate parameters were $\eta_1 = \eta_2 = 0.4$ and the initial variance was $\sigma^2 = 0.16$. After each epoch, η_1 and η_2 were decreased by 0.025 and σ^2 was decreased by 0.01. The lengths of the robot limbs were $l_1 = 0.5$ and $l_2 = 0.35$.

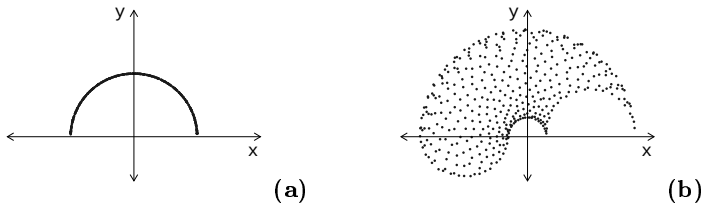

Figure 4: The sensory components of all learned body icons, $i = 1 \ldots \mathcal{I}$. (a) $\tilde{v}^i_{r_1}$ - elbow; (b) $\tilde{v}^i_{r_2}$ - wrist.

inverse function of the squared Euclidean distance between v_{r_2} and v_{ao} for all PEs, i.e.,

$$\xi^{ao} = \xi^{ao}(\mu) = \frac{1}{\|v_{ao} - v_{r_2}(\mu)\|^2} \tag{6}$$

The magnitude of each point in the potential field is computed in $\mathcal{S}$-space but using the body icon representation the field is imposed on $\mathcal{C}$-space. Figure 7 shows several trajectories defined by the end effector moving toward the goal from various starting positions. Note that in Figure 7b the placement of the attractor object is is outside the effective sphere of reach of the robot. In this case the tip of the manipulator moves to the point on the boundary of the reachable space that is closest to the goal.

To test the extensibility properties of the RBS model the same experiment was repeated with the robot holding a stick (Figure 5). In this case, the robot has two contact sensors C_1 and C_2 associated with its two body locations, L_{r_1} and L_{r_2}. The stick was modified to have three locations, L_{s_1}, L_{s_2}, and L_{s_3}, which are easily identifiable by the robot's vision system (Figure 5).

The *extended* sensory components of the body icons corresponding to the wrist (i.e., the attachment point) were computed as follows

$$\tilde{v}^i_{r_2} = \tilde{v}^i_{r_2} + \vec{y}^i_{r_2} \|v_s - v_{r_2}\| \tag{7}$$

where v_s stands for the image coordinates of one of L_{s_1}, L_{s_2}, or L_{s_3}. Because the stick is a linear extension of the second limb only one basis vector is necessary to compute each offset vector. The unit basis vectors, $\vec{y}^i_{r_2}$, are computed using the stored positions for the two robot body locations in all body icons as shown below

$$\vec{y}^i_{r_2} = \frac{\tilde{v}^i_{r_2} - \tilde{v}^i_{r_1}}{\|\tilde{v}^i_{r_2} - \tilde{v}^i_{r_1}\|} \tag{8}$$

Figures 6b, 6c, and 6d show the extended $\tilde{v}^i_{r_2}$ vectors for all body icons when each of the three tool locations are used in

the extension. Note how the extended reachability space differs from the original RBS representation shown in Figure 6a.

The potential field method can still be used to control the position of the stick: $\xi^{stick} = \xi^{stick}(\mu) = \frac{1}{\|v_{ao} - v_{r_2}(\mu)\|^2}$. In this case, however, $v_{r_2}(\mu)$ refers to the extended body icons computed using Formula 7. For example, the tip of the stick can be controlled using the same algorithm used to control the end effector if v_{s_3} is used in Formula 7 to compute the extended body icons. Figure 8 shows several trajectories defined by the tip of the stick as it moves toward the goal from various starting positions.

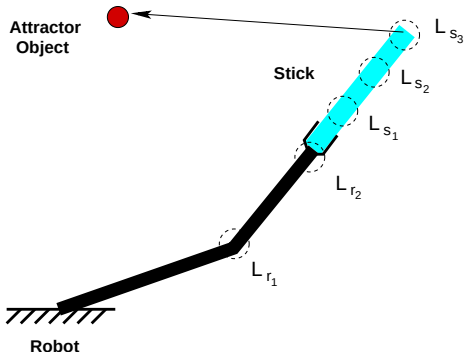

Figure 5: The robot from Figure 3a holding a stick. The stick has three locations, L_{s_1}, L_{s_2}, and L_{s_3}, that are identifiable by the robot's vision system.

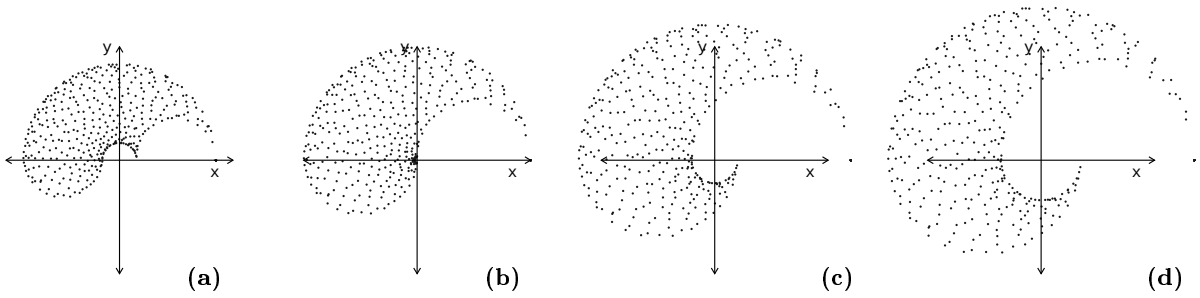

Figure 6: The figure shows the extended sensory components of the body icons after a stick is attached to the robot. In this case only the wrist components, $\tilde{v}^i_{r_2}$, are extended. (a) Original configuration before the stick is attached (same as in Figure 4b); (b), (c), and (d) Extended configurations when v_{s_1}, v_{s_2}, and v_{s_3} respectively are used in Formula 7.

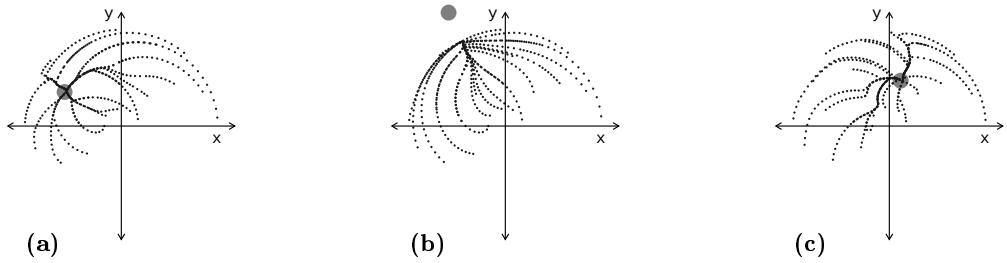

Figure 7: Trajectories defined by the movement of the end effector toward the attractor object starting from various initial positions. Note that in b) the attractor object is placed outside the space reachable by the robot.

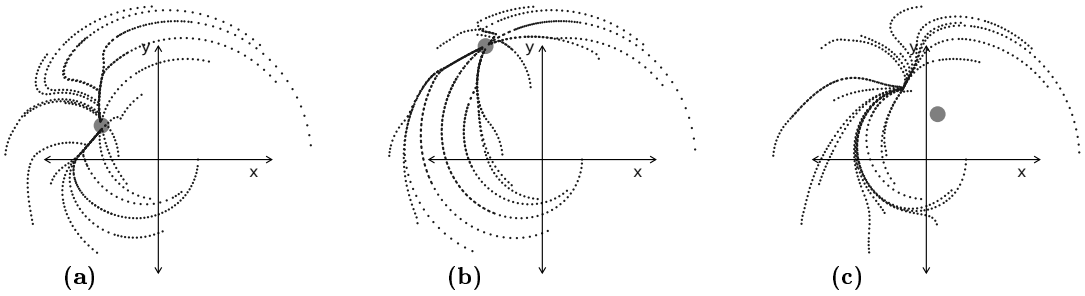

Figure 8: Trajectories defined by the movement of the tip of the stick toward the attractor object starting from various initial positions. The three positions of the attractor object are the same as in Figure 7. Note that in c) the attractor object is placed outside the space reachable with the tip of the stick.

6 Conclusions and Future Work

This paper introduced the notion of *extended robot body schema* and described a computational model that implements this notion. It was shown how the extensibility of the RBS can be achieved by combining visual, tactile, and proprioceptive sensors to extend the visual components of the body icons. As noted in Section 2, the results of the extension module are similar to the results observed by Iriki et al. (1996) in their experiments with monkeys. At this time, however, we do not claim that the proposed model is a model of how biological brains compute the extended body schema.

The model presented here has several advantages over traditional methods for robot control. First, the RBS model is learned from self observation during a motor babbling phase. Unlike world models, which are generally avoided by many robot architectures because they are often inaccurate and difficult to learn, the RBS represents a model of the robot which is significantly simpler to learn. Furthermore, this model is not likely to change over time and specialized routines can be used to learn it and to update it over time. Second, it provides the robot with a sensory-motor model of its own body that can also be used to control robot movements. Third, the RBS representation makes explicit the distinction between sensory stimuli coming from the environment and sensory stimuli coming from the robot which can potentially simplify the process of behavioral specification. And finally, through the process of extension the RBS can accommodate changes in the configuration of the robot triggered by attached objects and tools.

Several problems, however, remain to be addressed. First, the proposed approach makes the assumption that visually distinct locations on the surface of the robot body can be identified. Finding perceptual algorithms for autonomous selection of the robot body locations and their sensory stimuli is an important problem that needs to be addressed. Second, it is not clear what is the optimal number of body icons necessary for a given task. Also, it is not clear how many body locations are necessary in order to accommodate body extensions by objects with complicated geometries. And finally, it is important to find ways of extending the RBS that take into account the dynamics of the robot and the attached object. For example, a long stick may have the potential to extend the reach of the robot but if the stick is heavy this extension may not be achievable for some or all joint configurations of the robot.

References

S. Aglioti, N. Smania, M. Manfredi, and G. Berlucchi. Disownership of left hand and objects related to it in a patient with right brain damage. *NeuroReport*, 8:293–296, 1997.

R. Arkin. *Behavior-based robotics*. MIT Press, 1998.

M. Asada, K.F. MacDorman, H. Ishiguro, and Y. Kuniyoshi. Cognitive developmental robotics as a new paradigm for the design of humanoid robots. *Robotics and Automation*, 37:185–193, 2001.

G. Berlucchi and S. Aglioti. The body in the brain: neural bases of corporeal awareness. *Trends in Neuroscience*, 20(12): 560– 564, 1997.

A. Berthoz. *The brain's sense of movement.* Harvard University Press, 2000.

A. Berti and F. Frassinetti. When far becomes near remapping of space by tool use. *Journal of Cognitive Neuroscience*, 12(3):415–420, 2000.

A. Farné and E. Ládavas. Dynamic size-change of hand peripersonal space following tool use. *NeuroReport*, 11(8):1645–1649, June 2000.

J. Frederiks. Disorders of the body schema. In *Handbook of Clinical Neurology: Disorders of Speech Perception and Symbolic Behavior*, volume 4, pages 207–40. 1969.

J. J. Gibson. *The ecological approach to visual perception.* Houghton Mifflin, Boston, 1979.

M. Graziano, D. Cooke, and C. Taylor. Coding the location of the arm by sight. *Science*, 290:1782–1786, December 2000.

M. Graziano, C. Taylor, and T. Moore. Complex movements evoked by microstimulation of precentral cortex. *Neuron*, 30 May 2002.

H. Head and G. Holmes. Sensory disturbance from cerebral lesions. *Brain*, 34:102–254, 1911.

J-Y. Hervé, R. Sharma, and P. Cucka. Geometry of visual coordination. In *AAAI*, pages 732–737, 1991.

A. Iriki et al. Coding of modified body schema during tool use by macaque postcentral neurons. *Neuroreport*, 7:2325–2330, 1996.

A. Iriki et al. Self-images in the video monitor coded by monkey intraparietal neurons. *Neuroscience Research*, 40:163–173, 2001.

R. Melzack. Phantom limbs. *Scientific American*, (266):120–126, April 1992.

P. Morasso and V. Sanguineti. Self-organizing body-schema for motor planning. *Journal of Motor Behavior*, 27(1):52–66, 1995.

J. Paillard. The hand and the tool: The functional architecture of human technical skills. In *The Use of Tools by Human and Non-human Primates*, pages 36–46. Oxford University Press, 1993.

A. Pick. Störung der orientierung am eigenen körper. *Psychol. Forsch*, 1:303–318, 1922.

V. Ramachandran and D. Rogers-Ramachandran. Synaesthesia in phantom limbs induced with mirrors. *Proc. Royal Society London, Series B.*, 263(1369), Apr. 22 1996.

P. Schilder. *Das Körperschema.* Springer Verlag, Berlin, 1923.

S. Schultz. *Princeton Weekly Bulletin*, 90(26), April 30 2001.

R. Sharma, J-Y. Hervé, and P. Cucka. Dynamic robot manipulation using visual tracking. In *IEEE ICRA*, pages 1844–1849, 1992.

R. Sharma and H. Sutanto. Integrating configuration space and sensor space for vision-based robot motion planning. In *Workshop on the Algorithmic Foundations of Robotics*, pages 63–77, 1996.

D. Tiemersma. *Body Schema and Body Image: An Interdisciplinary and Philosophical Study.* Swets and Zeitlinger B. V., Amsterdam, 1989.

Y. Tsukamoto. Pinpointing of an upper limb prosthesis. *Journal of Prosthetics and Orthotics*, 12(1):5–6, 2000.

Y. Yoshikawa, H. Kawanishi, M. Asada, and K. Hosoda. Body scheme acquisition by cross map learning among tactile, image, and proprioceptive spaces. In *Proceedings of the Second International Workshop on Epigenetic Robotics*, 2002.